Impaired Retinal Differentiation and Maintenance in Zebrafish Laminin Mutants

Oliver Biehlmaier,[*,1,2,3] *Yuri Makhankov,*[1,2] *and Stephan C. F. Neuhauss*[*,1,2,3]

Purpose. To characterize morphologic and physiological alterations in the retina of three laminin mutant zebrafish, bashful (*bal*, lama1), grumpy (*gup*, lamb1), and sleepy (*sly*, lamc1), which were identified in forward genetic screens and were found to be impaired in visual functions.

Methods. Mutant larvae were observed for defects in visual behavior by testing their optokinetic response (OKR). In addition, electroretinograms (ERG) were measured and retinal morphology was examined by standard histology, immunocytochemistry, TUNEL assay, and electron microscopy.

Results. Both, *gup* and *sly* showed no OKR at any light intensity tested, whereas *bal* embryos showed some remaining OKR behavior at more than 40% of contrast. Consistent with the OKR result, *gup* and *sly* did not show an ERG response at any light intensity tested, whereas *bal* mutants exhibited small a- and b-waves at high light intensities. All three laminin mutants showed altered ganglion cell layers, optic nerve fasciculations, and lens defects. Again, *bal* showed the least severe morphologic phenotype with no additional defects. In contrast, both, *gup* and *sly*, showed severe photoreceptor outer segment shortening and synapse alteration (floating ribbons) as well as increased cell death.

Conclusions. Lamb1 and lamc1 chains play an important role in the morphogenesis of photoreceptors and their synapses. In contrast, lama1 is not involved in outer retina development. (*Invest Ophthalmol Vis Sci.* 2007;48:2887–2894) DOI: 10.1167/iovs.06-1212

Laminins are heterotrimeric glycoproteins that are composed of α, β, and γ chains. So far, 15 laminin isoforms have been identified in different tissues and at different developmental stages.[1,2] They can bind to integrins, dystroglycan, syndecans, and other cell surface molecules that act as their cellular receptors. Laminin proteins are crucial elements of the extracellular matrix and are known to be involved in central nervous system (CNS) development, in particular in forming and maintaining neuronal contacts, both during development and in the adult. This is also the case in the retina, where laminins are present in many different compartments—namely, Bruch's membrane, the interphotoreceptor matrix, the external limiting membrane (ELM), the outer plexiform layer (OPL), inner plexiform layer (IPL), and inner limiting membrane (ILM).[3] Because of the presence in these retinal compartments, laminins are thought to play a central role in development and maintenance of photoreceptor structure and synaptic function.[3] In addition to their effects on the neural retina, it has been shown recently that laminins are crucial for lens development.[4–6]

In humans, mutations in laminin-encoding genes lead to severe diseases such as junctional epidermolysis bullosa,[7] congenital muscular dystrophy,[8] and Pierson syndrome,[9,10] a disease causing a severe nephrotic syndrome followed by early-onset end-stage renal disease accompanied by ocular impairments such as extreme nonreactive narrowing of the pupils and complex maldevelopment of the eyes, including lens abnormalities, atrophy of the ciliary muscle, corneal changes, and retinal alterations.

In the zebrafish, three laminin mutants, named bashful (*bal*; lama1), grumpy (*gup*; lamb1), and sleepy (*sly*; lamc1) have been identified due to their reduced body length and defects in notocord differentiation.[11–13] Anterior–posterior axon trajectory defects in the retinotectal projection are apparent in gup and sly mutant larvae after DiI and DiO labeling.[14] These two mutants were also identified in a screen for defects in visual behavior with defective optokinetic response (OKR), ERG, and retinal morphology.[15]

We describe the morphologic, behavioral, and electrophysiological alterations in the retinas of these mutants.

Methods

All experiments were conducted in compliance with the ARVO Statement for the Use of Animals in Ophthalmic and Vision Research.

Fish Maintenance and Breeding

Fish were maintained and bred as described elsewhere.[16] We used the zebrafish strains Tübingen (TÜ) and Tup Long Fin (TL).[17] grumpy (*gup*^{tg210}), sleepy (*sly*^{ti263a}), and bashful (*bal*^{tp82}) larvae were obtained by mating of identified heterozygous carriers, and the embryos were sorted according to their small body and eye size. A comparison of the strength of these alleles with the published data[5,12–14,18,19] suggests that the alleles used are functional null alleles. Embryos were raised at 28°C in E3 medium (5 mM NaCl, 0.17 mM KCl, 0.33 mM $CaCl_2$, and 0.33 mM $MgSO_4$) and staged according to development in days postfertilization (dpf).

Retinal Histology

Larvae were anesthetized at 4°C on ice before fixation. For light microscopy, they were then immediately fixed in 4% paraformaldehyde in 0.2 M phosphate buffer (PB; pH 7.4) for 1 hour (4°C). Larvae

From the [1]Department of Biology, Swiss Federal Institute of Technology (ETH) Zurich, and the [2]Brain Research Institute, University of Zurich, Zurich, Switzerland.

[3]Present address: Institute of Zoology, University of Zurich, Zurich, Switzerland.

Supported by the Swiss National Science Foundation (SCFN), the Velux Foundation (OB), and the EMBO Young Investigator Program (SCFN).

Submitted for publication October 9, 2006; revised February 26, 2007; accepted April 20, 2007.

Disclosure: **O. Biehlmaier**, None; **Y. Makhankov**, None; **S.C.F. Neuhauss**, None

The publication costs of this article were defrayed in part by page charge payment. This article must therefore be marked "*advertisement*" in accordance with 18 U.S.C. §1734 solely to indicate this fact.

*Each of the following is a corresponding author: Oliver Biehlmaier, Swiss Federal Institute of Technology (ETH) Zurich, Department of Biology, and the Brain Research Institute, University of Zurich, Winterthurerstrasse 190, CH 8057 Zurich, Switzerland; biehlmaier@hifo.unizh.ch.

Stephan C. F. Neuhauss, University of Zurich, Institute of Zoology, Winterthurerstrasse 190, CH 8057 Zurich, Switzerland; stephan.neuhauss@zool.unizh.ch.

for electron microscopy (EM) were fixed in 1% paraformaldehyde and 2.5% glutaraldehyde in 0.1 M PB overnight. For standard histology, fixed larvae were dehydrated in a graded series of ethanol-water mixtures and embedded in resin (Technovit 7100; Kulzer, Wehrheim, Germany). Microtome sections (3 μm) were prepared and mounted on slides (SuperFrost Plus; Menzel-Gläser, Braunschweig, Germany). They were then air dried at 60°C, stained with Richardson solution (1% azure, 1% methylene blue, and 1% borax in deionized water), and coverslipped with mounting medium (Entellan; Merck, Darmstadt, Germany).

Quantifications

Photoreceptor Layer: Thickness Quantification. Toluidine blue-stained resin-embedded sections with a thickness of 5 μm were evaluated by using bright-field optics. In each larva, we measured the photoreceptor layer thickness as the distance, from the inner end of the photoreceptor soma to Bruch's membrane. In each laminin mutant, three sections from two to three different fish were quantified. In each section, 10 loci in proximity to the optic nerve were analyzed. Thus, 20 to 30 loci were analyzed per replicate. The bar graphs were designed and the statistic tests performed in commercial software (Prism 4.03; GraphPad, San Diego, CA). Significance between *bal*, *gup*, and *sly* retinas was determined by one-way ANOVA and the Tukey post hoc test (Prism; GraphPad, San Diego, CA).

Lens Phenotype Quantification in the *bal* Mutant. Toluidine blue–stained, resin-embedded sections and unstained cryostat sections visualized by differential interference contrast (DIC) optics were screened for lens phenotypes in 35 eyes of 19 different *bal* larvae.

Electron Microscopy

The EM-fixed larvae were washed in 0.1 M PB for 2 hours and postfixed in 1% osmium tetroxide for 1 hour, 20 minutes. After they were rinsed in 0.1 M PB, the specimens were dehydrated in a graded series of ethanol-water mixtures up to 100% ethanol. After preinfiltration in 1:1 100% ethanol/embedding resin (Fluka, Buchs, Switzerland), larvae were infiltrated in pure embedding resin overnight. Larvae were then positioned in embedding capsules (Beem caps; Canemco & Marivac, Canton de Gore, Quebec, Canada) with fresh resin and polymerized at 60°C for approximately 16 hours. Ultrathin (60 nm) transverse sections were prepared, contrasted with lead citrate, examined, and photographed with a transmission electron microscope (model EM 900; Carl Zeiss Meditec, Oberkochen, Germany).

Cell Death Detection

Fixed larvae were cryoprotected in 30% sucrose for at least 4 hours. Entire larvae were then embedded in tissue-freezing medium (Cryomatrix; Reichert-Jung, Vienna, Austria) and rapidly frozen in liquid N_2. Cryosections (25 μm thick) were cut at −20°C, mounted on slides (Super Frost Plus; Menzel-Gläser; Braunschweig, Germany), air dried at 37°C for at least 2 hours, and stored at −20°C until further use. For cell death detection, the slides were thawed, and apoptosis was detected by using the TUNEL (terminal deoxynucleotidyl transferase [TdT]mediated deoxyuridinetriphosphate [dUTP] nick end-labeling) method,[20] as previously described.[21]

Immunohistochemistry

Fixed larvae were cryoprotected in 30% sucrose for at least 4 hours. Entire larvae were then embedded in tissue-freezing medium (Cryomatrix; Reichert-Jung) and rapidly frozen in liquid N_2. Cryosections (15 μm thick) were cut at −20°C, mounted on slides (Super Frost Plus; Menzel-Gläser), air dried at 37°C for at least 2 hours, and stored at −20°C until further use. For immunohistochemistry, the slides were thawed, washed three times in PBS (50 mM, pH 7.4), and incubated in blocking solution (BS; 10% NGS and 1% BSA in 0.3% PBS/Triton X-100) for 1 hour. Sections were then incubated overnight in primary antibody in BS at 4°C. The immunolabeling was visualized by using Alexa488-conjugated anti-mouse IgG or anti-rabbit IgG (1:1000; Invitrogen-Molecular Probes, Basel, Switzerland) as a secondary antibody. The following primary antibodies were used for immunostaining: monoclonal mouse anti-zpr1 (1:20; University of Oregon Stock Center), monoclonal mouse anti-glutamine synthetase (GS, 1:700; Chemicon, Harrow, UK), and polyclonal rabbit anti-syntaxin3 (Synt3, 1:400; Alamone Laboratories, Jerusalem, Israel).

After the immunostaining, the slides were coverslipped and analyzed under a fluorescence microscope (Axioscope; Carl Zeiss Meditec, with AxioVision 4 as the imaging software).

OKR Measurements

Visual performance was assessed by measuring the OKR as previously described.[22] To measure eye velocity, single larvae were placed dorsal-side-up in the center of a Petri dish (35 mm diameter) containing 3% prewarmed (28°C) methylcellulose. Moving sine-wave gratings were projected by a linearized HP vp6111 projector onto a screen within the visual field of the larva. The apparent distance from the larva's right eye to the screen was 4.65 cm, and the projection size on the screen was 8 × 6 cm, subtending a visual angle of 65.6° horizontally and 53.1° vertically. Eye movements were triggered by the visual stimulation and recorded by an infrared-sensitive CCD camera. Custom-written software (based on LabView IMAQ ver. 5.1; National Instruments, Austin, TX) was used to control the stimulation and the camera and to analyze the resulting images. Contrast sensitivity functions for wild-type (wt) and laminin mutant larvae were measured as eye velocity as a function of the spatial frequency of the moving grating with alternating movement direction (0.33 Hz). The averaged eye velocity for each spatial frequency was calculated by integration of eye-velocity traces. Graphs were designed and the statistical tests performed with commercial software (Prism 4.03; GraphPad). Significant differences between *bal* ($n = 5$), *gup* ($n = 5$), *sly* ($n = 5$), and their respective siblings ($n = 5$) were determined by a two-way ANOVA and Bonferroni post hoc test.

Electroretinographic Recordings

Electroretinograms (ERGs) were recorded from 5 dpf larvae as previously described.[23] All specimens were dark-adapted for 30 minutes before positioning them in the recording chamber. Each larva was placed on the surface of a moist sponge with E3 medium and paralyzed by directly applying a droplet of the muscle relaxant (Esmeron; 0.8 mg/mL in larval medium; Organon Teknika, Eppelheim, Germany). Light flashes of 200 ms duration were separated by 7-second intervals. Unattenuated irradiation at the position of the subject as measured by a photometer with photopic sensitivity profile was 5.7 mW/cm^2.

A virtual instrument (VI) (NI LabVIEW ver. 5.1; National Instruments) was used to control the stimulation and to record ERG traces on computer. Sampling was performed in buffered acquisition mode with a sampling rate of 1000 Hz, and responses were averaged between five acquisitions.

Results

Laminin Mutations Lead to Alterations in Retinal Morphology

In previous studies, it has been shown that laminin mutations encoding for laminin α1, β1, and γ1 are important both for notochord differentiation and for proper intersegmental blood vessel formation.[11–13,18] In addition, defects in vision have been reported for β1, and γ1 laminin mutant larvae.[15] To assess the general retinal morphology of these laminin deficient fish, we analyzed laminin mutant and wt retinas with standard histologic techniques (Figs. 1A–D) at 5 dpf. All three laminin mutants showed similar retinal alterations: They pos-

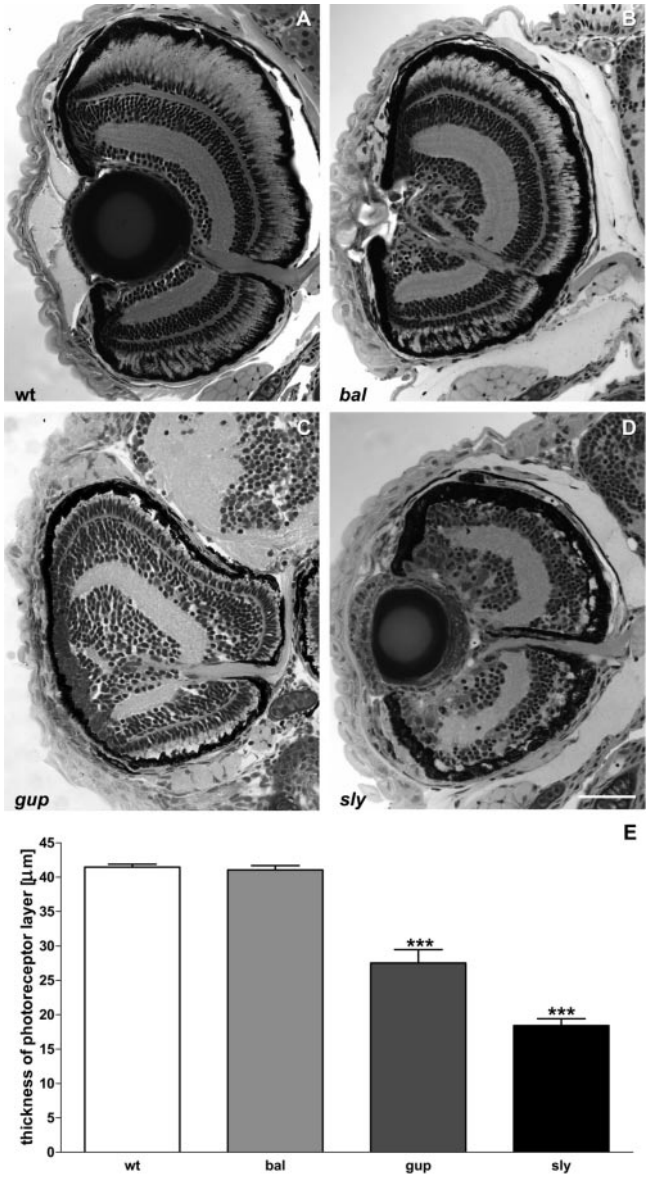

FIGURE 1. Transverse sections through wt (**A**) and laminin mutant retinas (**B–D**) and quantification of the respective photoreceptor layer thickness (**E**). The *bal* mutant (**B**) had no lens. The GCL and optic nerve were clearly altered. However, remaining parts of the retina were morphologically normal. The *gup* and *sly* mutants (**C**, **D**) also lacked or had smaller lenses and also showed GCL and optic nerve alterations. In addition, the photoreceptors were severely shortened, especially in *sly*. Quantification of photoreceptor thickness (**E**) reveals no differences between wt and *bal*, but significant differences between wt and *gup* and wt and *sly* (***$P < 0.001$; Tukey post hoc test).

sessed either no lens (Figs. 1B, 1C) or a small lens (Fig. 1 D). In addition, the ganglion cell layer (GCL) was affected in all three mutants (Figs. 1B–D). The classic morphology at 5 dpf, with approximately three rows of ganglion cells (GCs) and the optic nerve entering in one big bundle of nerve fibers was broken up. GCs clearly formed more than three rows of cell bodies and were arranged in a less orderly fashion (Figs. 1B–D), probably because of the available space left by the reduced or lacking lens. In the wt, fasciculation of GC axons became apparent first at the exit point of the GC layer, where they formed the optic nerve growing toward the optic nerve head in a tight, fasciculated bundle (Fig. 1A). In contrast, several smaller fascicles originating from GCs of the mutant GCL projected toward the normally fasciculated optic nerve.

Besides these common pathomorphologies, β1 and γ1 mutants showed remarkable shortening of photoreceptor (PhR) outer segments (Figs. 1C, 1D). Quantification of the PhR layer thickness revealed significantly reduced photoreceptors in the *gup* and *sly* mutants (Fig. 1E). In comparison to the thickness measured in wt siblings (41.5 $\pm$ 0.40 μm), the PhR layer thickness in *gup* was significantly reduced to 27.5 $\pm$ 2.0 μm and in *sly* to 18.4 $\pm$ 1.0 μm. In contrast, *bal* mutants showed wt-like PhR layer thickness of 41.0 $\pm$ 0.6 μm.

To determine the extent to which the photoreceptors and their synapses are affected by the respective laminin mutations we used immunohistochemistry to label double cones (zpr1-labeling) and ribbon synapses (Syntaxin 3;[24]) specifically in the OPL at 5 dpf. All three mutants showed zpr1-labeling. However, whereas the labeling in *bal* mutants (Fig. 2B) was almost identical with that in the wt (Fig. 2A), *gup* (Fig. 2C) and *sly* (Fig. 2D) larvae expressed zpr1-labeling only in double cone inner segments and somata, thus suggesting outer segment degeneration. As it is known that laminins are highly expressed in the synaptic layers of the retina,[3] we wanted to know whether the different laminin mutations would affect the expression of specific synaptic markers of the OPL. Therefore, we labeled ribbon synapses by using a Syntaxin 3 antibody. In this staining, ribbon synapses were labeled to the same extent in wt and all three laminin mutants (Fig. 2E–H), thus indicating that the remaining synapses between photoreceptors and second order neurons still possess normal ribbon synapses.

Ultrastructure of Photoreceptors and Their Synapses in Laminin Mutants

Knowing that photoreceptors are affected by the laminin mutations in *gup* and *sly*, we examined the ultrastructure of the outer retina by using electron microscopy to gain further insight. Again, the situation in the *bal* mutant outer retina at 5 dpf (Fig. 3B) resembled very much the situation in wt larvae (Fig. 3A). *Bal* mutants showed normally elongated cone outer segments and healthy RPE cells. As expected from the immunohistochemical data, outer segments in *gup* (Fig. 3C) and *sly* (Fig. 3D) are strongly shortened. In addition to this photoreceptor defect, *gup* larvae express an altered RPE with fewer melanin granules and abundant vacuoles in the RPE (Fig. 3D). However, Bruch's membrane, a structure where laminin-1 is deposited[6] is unaffected by the mutations (Figs. 3B–D).

Next, we analyzed the photoreceptor ribbon synapse at the ultrastructural level. We identified classic cone pedicles including triads of invaginating horizontal (HC) and bipolar (BC) cell dendrites adjacent to respective ribbon synapses in wt (Fig. 3E) and *bal* larvae. However, invaginating dendrites were reduced and instead of classical "triade associated" ribbons, floating ribbons were frequently observed in *gup* larvae (Fig. 3G). The photoreceptor synapse of *sly* mutant larvae is even more strongly affected with only very few or no ribbons and hardly any invaginating dendrites formed (Fig. 3H). Moreover, the classic bell-shaped structure of cone pedicles was lost in the *sly* mutant.

Retinal Cell Death in Laminin Mutants

We next asked whether the retinal defects in these mutants are associated with an increase in apoptotic cell death by applying the TUNEL assay.[20] The number of TUNEL-positive cells detected in 5 dpf wt (Fig. 4A) and *bal* (Fig. 4B) mutant larvae was

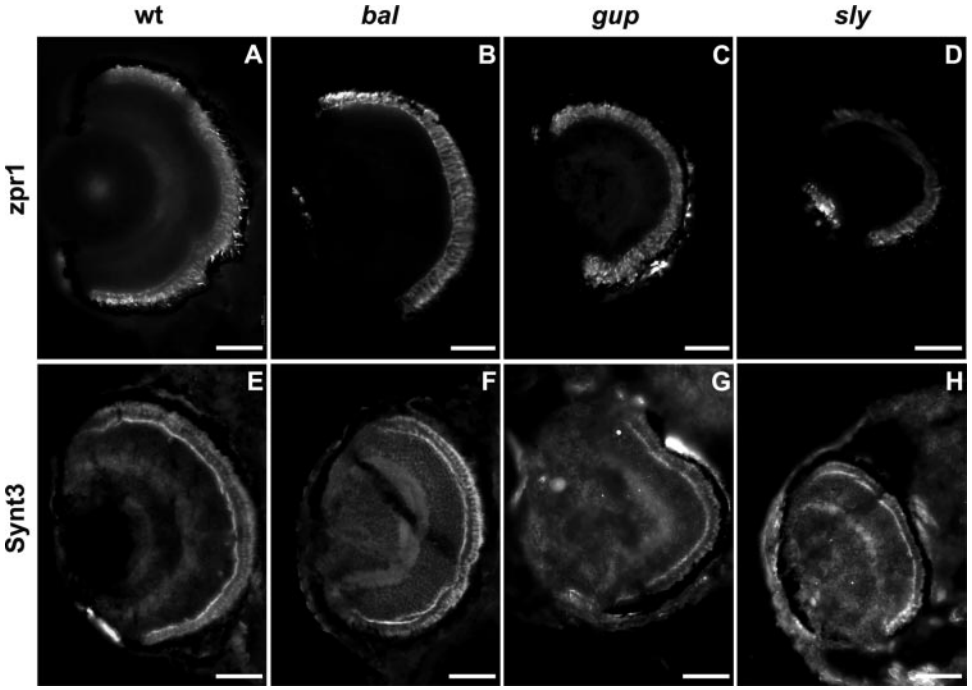

FIGURE 2. Double cone labeling (zpr1; **A–D**) and ribbon synapse labeling (syntaxin 3; **E–H**) in transverse sections of wt and laminin mutant larvae at 5 dpf. Entire double cones, including the inner and outer segments, were clearly labeled in wt (**A**) and *bal* (**B**) larvae. In contrast, zpr1 labeling was restricted to the inner segments and somata in *gup* (**C**) and *sly* (**D**) larvae. Ribbon type synapses were labeled to the same extend in wt (**E**) as well as in all mutant retinas (**F–H**). Scale bar, 50 μm.

very low with no more than one to three labeled cells per section and thus corresponded closely to the rate reported from zebrafish normal development.[21] In contrast, the amount of cell death observed in *gup* (Fig. 4C) and *sly* (Fig. 4D) was very high, showing numerous dying cells all over the retina. In the *sly* mutant, most of the apoptotic cells were labeled in the outer nuclear layer (ONL), thus suggesting severe photoreceptor degeneration (Fig. 4D).

Cells of the Inner Retina in Laminin Mutant Zebrafish

To examine whether the alterations induced by the laminin defect also affect neurons of the inner retina, we labeled several cell populations by using specific antibodies: 5e11 to label amacrine cells, TH to label dopaminergic amacrine cells, cPKCβ to label mixed rod cone bipolar cells, and GS to label Müller cells (MCs). All these cell types were clearly identified by the respective antibody in the mutant retinas (data not shown) and the labeling did not show any altered morphology concerning the intensity and localization of the immunolabeling in the respective individual cells. However, GS staining was altered in all three mutant retinas with regard to the Müller cell end feet (Fig. 5). Despite a normal morphology with clearly labeled somata and radial processes spanning from the OLM to the ILM, the staining pattern was clearly altered in all three mutants at the level of the ILM, where the mutants (Figs. 5B–D) did not form a regularly shaped margin between the vitreous and the GCL,

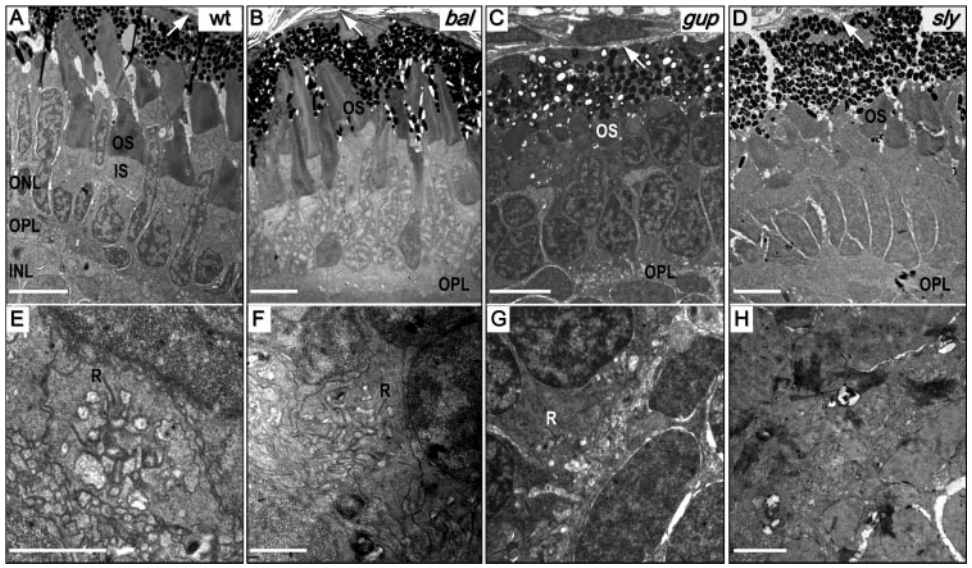

FIGURE 3. Transmission electron microscopy of transverse sections of the photoreceptor layer (**A–D**) and OPL (**E–H**) in wt and laminin mutant larvae at 5 dpf. Photoreceptor layer: (**A**) In the 5-dpf wt, photoreceptor outer segments (OS) were elongated and melanin-filled granules were clearly visible in the RPE. (**B**) In the 5-dpf *bal* mutant, OS were normally elongated in *bal* and RPE pigmentation was normal. Both (**C**) *gup* and (**D**) *sly* showed strongly reduced OS length and melanin granules with fainter pigmentation. Bruch's membrane was identifiable in wt and in all three laminin mutants (**A–D**, *arrows*). Synaptic layer: wt (**E**) and *bal* (**F**) showed classic cone pedicles with triads built by invaginating horizontal and bipolar cell dendrites and ribbon type synapses (R). (**G**) *gup* did not show normal triads: dendritic invagination was reduced and ribbons (R) were floating. (**H**) *sly* showed very few to no ribbons and very few invaginating dendrites. In addition, the classic bell-shaped morphology of cone pedicles was lost. Scale bars: (**A–D**) 5 μm; (**E–H**) 1 μm.

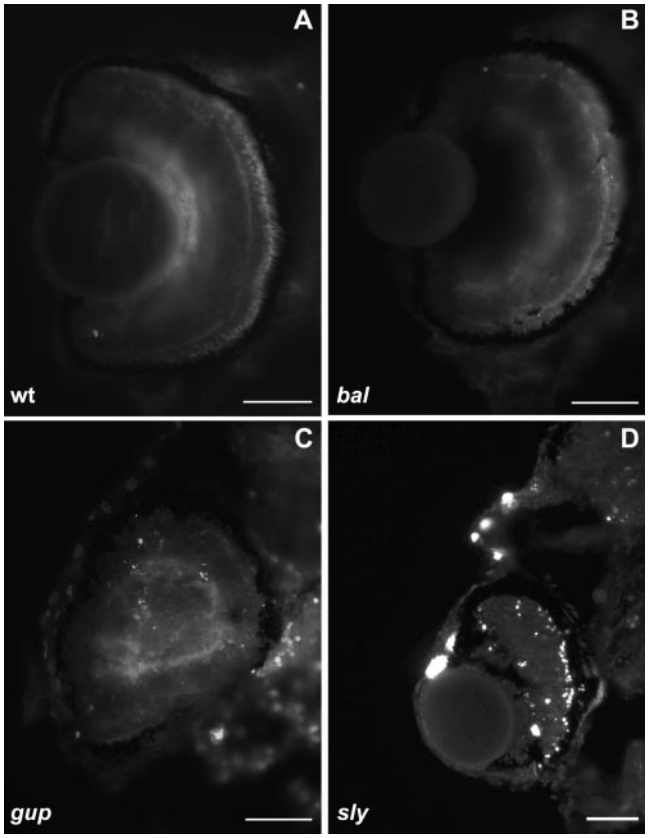

FIGURE 4. TUNEL staining in transverse sections of wt and laminin mutant larvae at 5 dpf. (**A**) The wt siblings showed only a few TUNEL-positive cell bodies. (**B**) The *bal* larvae showed a slight increase in apoptotic cells in the OPL. The *gup* (**C**) and especially the *sly* (**D**) larvae exhibited strongly increased cell death all over the retina, with the highest number of apoptotic cells in the ONL. Scale bars, 50 μm.

as was seen in their wt siblings (Fig. 5A). In contrast, close examination of individual Müller cells clearly showed that Müller end feet of all three laminin mutants terminated irregularly at different depths of the inner retina (Fig. 5B′–D′) thereby not building any separating membrane between the neuronal and the vitreal part of the retina. Taking into account that the ILM is composed by Müller glia end feet and ECM components[25] it is very much likely that the altered composition of the ECM leads to the breakup of the regular Müller end feet pattern.

Contrast Sensitivity and Retinal Signal Transmission in Laminin Mutants

To assess the impact of the described morphologic changes on vision, we measured contrast sensitivity of the OKR, a behavioral assay for visual performance[22]and ERG, a electrophysiological assessment of outer retinal function.[23]

Contrast sensitivity of all three laminin mutant larvae was severely reduced compared with that in respective wt siblings (Fig. 6; bootstrap resampling test, $P < 0.05$). However, the *bal* mutant (Fig. 6A) showed some residual OKR at light intensities of 50%, 70%, and 100%, thus suggesting that *bal* mutants are still able to see at higher light intensities.

To obtain insight in the overall physiology of the mutated eyes, we examined the ERGs of 5 dpf laminin mutant larvae and their wt siblings (Fig. 7). In accordance with the above described morphologic findings, *bal* mutants showed reduced but still clearly measurable ERG-signals (Fig. 7A). In contrast, both, *gup* and *sly* mutants did not show any remaining signal at any light intensity measured (Figs. 7C, 7E). These data are consistent with the behavioral analysis, indicating that *bal* mutants are able to see, whereas *gup* and *sly* are completely blind.

Given the nearly normal ERG in *bal* larvae, we hypothesized that the poor visual performance in the behavioral assay is due to defects in the retina and the lens. A small or degenerated lens should have a severe impact on visual behavior but should compromise the ERG only slightly.

DISCUSSION

In this study, we describe the retinal phenotype of three different laminin mutants, *bal* (lama1), *gup* (lamb1), and *sly* (lamc1) that had been previously described to have defects in notochord differentiation and intersegmental blood vessel formation.[11–13,18] All three laminin mutants showed an altered GCL and optic nerve and lens defects. The *bal* mutant did not show any other morphologic alterations, whereas *gup* and *sly* showed severe degeneration at the level of photoreceptors and synapses. In addition, no OKR and no ERG were detectable in *gup* and *sly* larvae, whereas *bal* homozygous showed some remaining OKR and a clear ERG at high contrast levels.

According to our results, a mutation in the lama1 gene encoding for the α1 laminin chain (*bal*) leads to defective laminin111 (formerly known as laminin 1; see Ref. 26) and defective laminin121 but leaves all other 13 known laminins unaffected. In contrast, mutations in lamb1 and lamc1 lead to

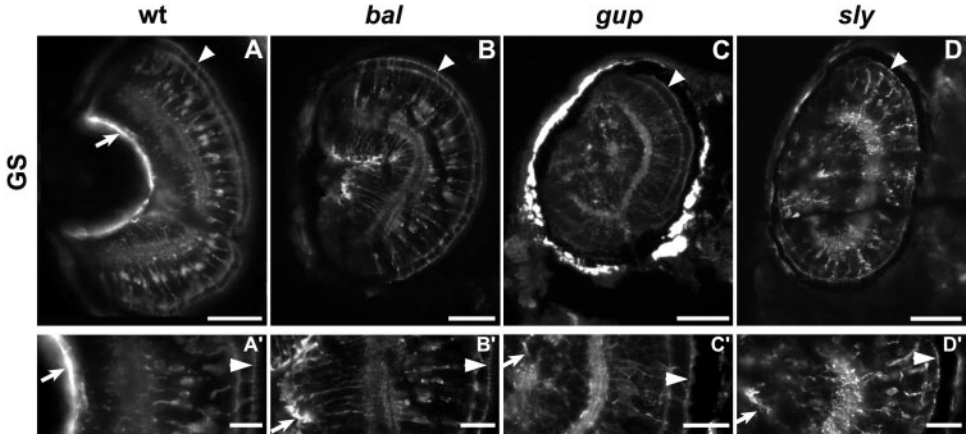

FIGURE 5. Müller cell labeling (GS; **A–D**) in transverse sections of wt and laminin mutant larvae at 5 dpf. (**A**) Classic GS labeling showing Müller cell soma and radial processes that terminate by building up the outer (OLM, *arrowhead*) and inner limiting membrane (ILM, *arrow*). (**B–D**, **B′–D′**) In the mutants Müller cell soma, radial processes, and OLM (*arrowheads*) were still visible, however, a continuous ILM was not discernible any more (*arrows*). Scale bar: (**A–D**) 50 μm; (**A′–D′**) 20 μm.

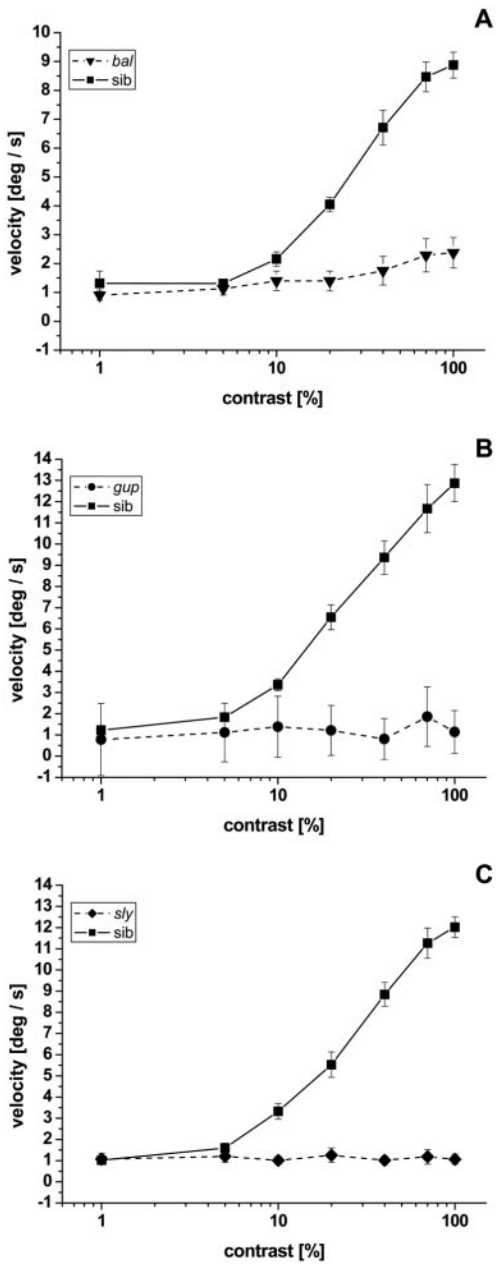

FIGURE 6. OKR of wt siblings versus laminin mutants at 5-dpf depicted as eye velocity as a function of stimulus spatial frequency (**A–C**). The OKR was significantly reduced in all three laminin mutants. (**A**) The *bal* mutants showed some remaining contrast sensitivity at higher contrast levels (>20%), whereas *gup* and *sly* mutants (**B**, **C**) were completely blind as they had lost all their contrast sensitivity and did not show any measurable OKR.

malformation of six different laminins in *gup* and 10 in *sly*, respectively.

Studies of the role of laminins in the zebrafish eye[4,5] have shown that a defect in laminin expression leads to alterations in lens morphology. Semina et al.[4] recently showed that lama1 mutant zebrafish show disrupted lens development with subsequent lens degeneration. The same was shown for lama1 knockdowns generated by using morpholino antisense oligonucleotides.[5] In addition to theses findings, Lee and Gross[6] showed that retroviral insertional mutations in lamb1 and lamc1 also lead to severe lens defects. In the present study we showed that lama1, lamb1, and lamc1 mutants have severe lens defects, varying from small lenses to no lenses. This deficiency is likely to be due to a compromise in lens capsule integrity.[6] However, because we still found lenses in some of the mutant eyes we suggest that the lense capsule defect leads to defective lens formation during early development, and later on, to a complete clearing of the lens from the laminin mutant eye.

In the OKR and ERG experiments, *bal* showed wt-like ERG but OKR responses only at high light intensities. We think that this difference in behavioral/functional performance in *bal* is caused by the altered lens morphology and the resultant low image quality on the mutant retina. In contrast, *gup* and *sly* did not show any measurable signals in any of the two functional tests due to the pathologically altered morphology of their photoreceptors that show shortened and degenerating outer segments, altered synapse ultrastructure, and thus impaired synaptic transmission. Similar phenotypes were observed in lamb2 chain–deficient mice.[27] However, in contrast to *gup* and *sly*, lamb2 chain–deficient mice still show a measurable a-wave, as well as other zebrafish mutants with alterations in photoreceptors and their synapses such as lazy eyes[28] and no OKR.[29] Therefore, we suggest that the photoreceptor alterations in lamb1 and lamc1 mutant zebrafish lead to a more severe deterioration of photoreceptor function and signal transmission than that observed in beta2 chain–deficient mice and other zebrafish mutants. This hypothesis is strengthened by the proven localization of different laminin chains, respectively special laminin trimers at different parts of the retinal tissue[3] (e.g., laminin332 in the interphotoreceptor matrix and OPL of the developing rat retina or lama1, lamb1, and lamc1 in the ILM and in Bruch's membrane) where they fulfill tissue specific functions. Thus, we suggest that lamb1 and lamc1 play a crucial role for the development and maintenance of the photoreceptors and their synapses, whereas lama1 does not or is functionally compensated by lama5, which is likely to be expressed in this retinal region as well.[3]

We found severe disorganization of the GCL and optic nerve in all three laminin mutants examined in the present study. Similar phenotypes have been described in other publications on laminin mutant[4,6] or morphant[5] zebrafish. There are two possible reasons for the GCL defect: One is that the malformation of the GCL may simply be associated with the fact of the reduced or lacking lens in the laminin mutants. Semina et al.[4] tested this hypothesis by comparing lama1 mutants to embryos in which the lens vesicle had been surgically removed. Their results suggests that many of the anterior and posterior ocular defects in the lama1 mutant are independent of the lens degeneration and, therefore, we suggest that this also holds true for the lama1, lamb1, and lamc1 mutants of our present study. The second hypothesis to explain the GCL defect is that the lack of any of the α-, β-, or γ-chains needed to build up the heterotrimeric laminin111 protein affects the structural integrity of the ILM. This membrane is known to contain laminin111.[3] Because of the interdependency between the laminins and the Müller cells in building up the ILM,[25] this change in structural integrity influences the termination locus of Müller cell end feet and in consequence the GCL lamination. This hypothesis is supported by reports of similar GCL alterations in other zebrafish laminin mutants[4,6] and morphants.[5] Therefore, a malformed ILM probably leads to a deteriorated GCL.

In conclusion, we found that lama1, lamb1, and lamc1 mutations lead to lens defects and morphologic alterations of the GCL and the optic nerve, whereas only lamb1 and lamc1 mutations lead to severe photoreceptor dysfunction.

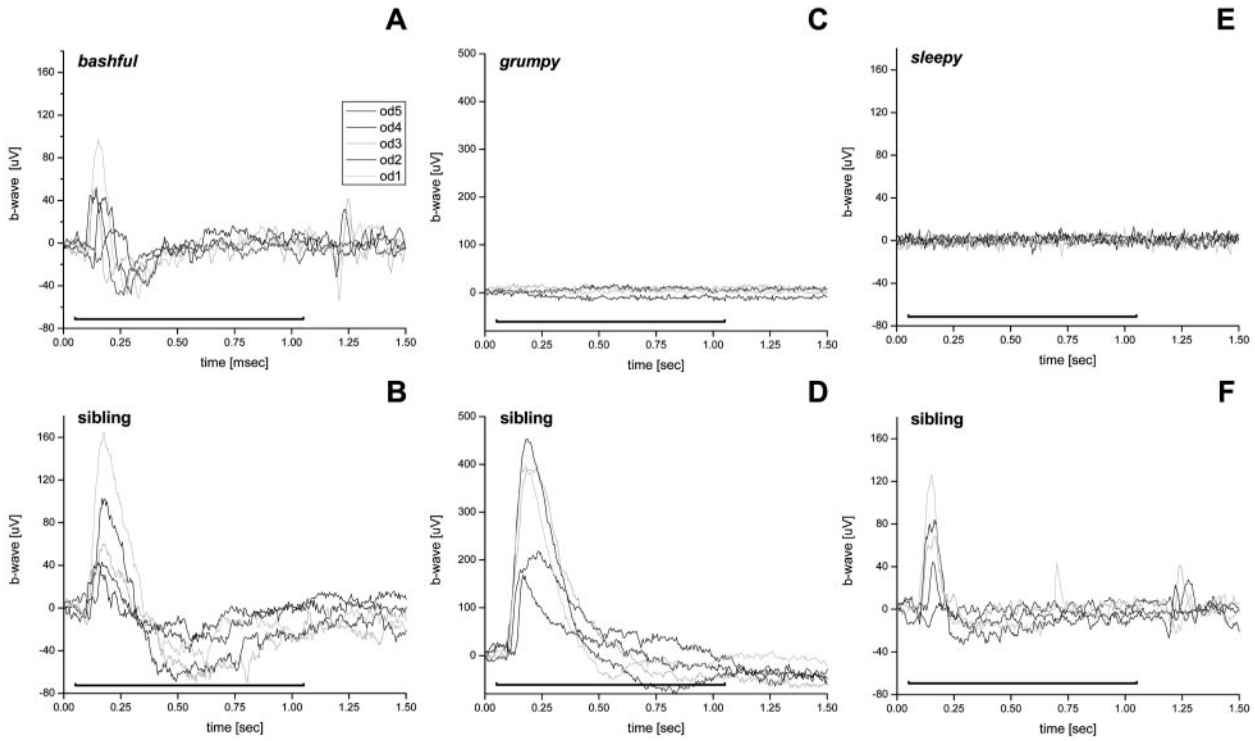

FIGURE 7. ERG recordings from dark-adapted laminin mutants and their wt siblings at different light intensities (OD 1–5) at 5 dpf. (**A**) The *bal* mutant showed a classic ERG at higher light intensity. The *gup* (**C**) and *sly* (**E**) mutants are completely blind, as they showed no ERG signal.

The affected retinal tissues are located in the retinal compartments known to contain laminin proteins in rodents, such as Bruch's membrane, the interphotoreceptor matrix, and the ELM, OPL, IPL, and ILM.[3] The lack or mutation of one chain of a trimeric laminin protein leads to developmental malformation and/or degeneration in the respective retinal compartments such as the photoreceptors, the OPL, or the GCL. As the mutation in the lama1 chain (*bal*) affects only the lens and the GCL and leaves other layers normal, we favor the idea that lama1 chains are not involved in outer retina development and maintenance or may be replaced by lama5 or other lama chains to compensate for the absent lama1 chain. The recent study by Semina et al.[4] furthers this hypothesis by showing that other alleles of lama1 mutation show similar phenotypes, affecting the GCL and lens, such as bal^{tp82}. Thus, all three laminin chains examined in this study are crucial in the formation of a proper ILM and a normal GCL, but only lamb1 and lamc1 are vital for photoreceptor development and maintenance. Finally, the outcome of this hypothesis is that the location of the respective laminin chains throughout the zebrafish retina correlates nicely with the laminin chain distribution suggested by Libby et al.[27] in the rat retina.

Acknowledgments

The authors thank Jeffrey Gross and Brian Perkins for helpful criticism and suggestions on the manuscript and Ticiana Jametti for helping with the GS staining.

References

1. Suzuki N, Yokoyama F, Nomizu M. Functional sites in the laminin alpha chains. *Connect Tissue Res*. 2005;46:142–152.
2. Tunggal P, Smyth N, Paulsson M, Ott MC. Laminins: structure and genetic regulation. *Microsc Res Tech*. 2000;51:214–227.
3. Libby RT, Champliaud MF, Claudepierre T, et al. Laminin expression in adult and developing retinae: evidence of two novel CNS laminins. *J Neurosci*. 2000;20:6517–6528.
4. Semina EV, Bosenko DV, Zinkevich NC, et al. Mutations in laminin alpha 1 result in complex, lens-independent ocular phenotypes in zebrafish. *Dev Biol.* 2006;299;63–77.
5. Zinkevich NS, Bosenko DV, Link BA, Semina EV. Laminin alpha 1 gene is essential for normal lens development in zebrafish. *BMC Dev Biol*. 2006;6:13.
6. Lee J, Gross JM. Laminin β1 and γ1 containing laminins are essential for basement membrane integrity in the zebrafish eye. *Invest Ophthalmol Vis Sci*. 2007;48:2483–2490.
7. Timpl R. Macromolecular organization of basement membranes. *Curr Opin Cell Biol*. 1996;8:618–624.
8. Arahata K, Ishii H, Hayashi YK. Congenital muscular dystrophies. *Curr Opin Neurol*. 1995;8:385–390.
9. Pierson M, Cordier J, Hervouuet F, Rauber G. An unusual congenital and familial congenital malformative combination involving the eye and kidney. *J Genet Hum*. 1963;12:184–213.
10. Zenker M, Pierson M, Jonveaux P, Reis A. Demonstration of two novel LAMB2 mutations in the original Pierson syndrome family reported 42 years ago. *Am J Med Genet A*. 2005;138:73–74.
11. Odenthal J, Haffter P, Vogelsang E, et al. Mutations affecting the formation of the notochord in the zebrafish, Danio rerio. *Development*. 1996;123:103–115.
12. Parsons MJ, Pollard SM, Saude L, et al. Zebrafish mutants identify an essential role for laminins in notochord formation. *Development*. 2002;129:3137–3146.
13. Stemple DL, Solnica-Krezel L, Zwartkruis F, et al. Mutations affecting development of the notochord in zebrafish. *Development*. 1996;123:117–128.
14. Karlstrom RO, Trowe T, Klostermann S, et al. Zebrafish mutations affecting retinotectal axon pathfinding. *Development.* 1996; 123(suppl):427–438.

15. Neuhauss SCF, Biehlmaier O, Seeliger MW, et al. Genetic disorders of vision revealed by a behavioral screen of 400 essential loci in zebrafish. *J Neurosci*. 1999;19:8603–8615.
16. Mullins MC, Hammerschmidt M, Haffter P, Nusslein-Volhard C. Large-scale mutagenesis in the zebrafish: in search of genes controlling development in a vertebrate. *Curr Biol*. 1994;4:189–202.
17. Haffter P, Granato M, Brand M, et al. The identification of genes with unique and essential functions in the development of the zebrafish, Danio rerio. *Development*. 1996;123:1–36.
18. Pollard SM, Parsons MJ, Kamei M, et al. Essential and overlapping roles for laminin alpha chains in notochord and blood vessel formation. *Dev Biol*. 2006;289:64–76.
19. Scott A, Stemple DL. Zebrafish notochordal basement membrane: signaling and structure. *Curr Top Dev Biol*. 2005;65:229–253.
20. Gavrieli Y, Sherman Y, Ben-Sasson SA. Identification of programmed cell death in situ via specific labeling of nuclear DNA fragmentation. *J Cell Biol*. 1992;119:493–501.
21. Biehlmaier O, Neuhauss SC, Kohler K. Onset and time course of apoptosis in the developing zebrafish retina. *Cell Tissue Res*. 2001; 306:199–207.
22. Rinner O, Rick JM, Neuhauss SC. Contrast sensitivity, spatial and temporal tuning of the larval zebrafish optokinetic response. *Invest Ophthalmol Vis Sci*. 2005;46:137–142.
23. Makhankov YV, Rinner O, Neuhauss SC. An inexpensive device for non-invasive electroretinography in small aquatic vertebrates. *J Neurosci Methods*. 2004;135:205–210.
24. Morgans CW, Brandstatter JH, Kellerman J, Betz H, Wassle H. A SNARE complex containing syntaxin 3 is present in ribbon synapses of the retina. *JNeurosci*. 1996;16:6713–6721.
25. Wolburg H, Willbold E, Layer PG. Müller glia endfeet, a basal lamina and the polarity of retinal layers form properly in vitro only in the presence of marginal pigmented epithelium. *Cell Tissue Res*. 1991;264:437–451.
26. Aumailley M, Bruckner-Tuderman L, Carter WG, et al. A simplified laminin nomenclature. *Matrix Biol*. 2005;24:326–332.
27. Libby RT, Lavallee CR, Balkema GW, Brunken WJ, Hunter DD. Disruption of laminin beta2 chain production causes alterations in morphology and function in the CNS. *J Neurosci*. 1999;19:9399–9411.
28. Kainz PM, Adolph AR, Wong KY, Dowling JE. Lazy eyes zebrafish mutation affects Müller glial cells, compromising photoreceptor function and causing partial blindness. *J Comp Neurol*. 2003;463: 265–280.
29. Allwardt BA, Lall AB, Brockerhoff SE, Dowling JE. Synapse formation is arrested in retinal photoreceptors of the zebrafish *nrc* mutant. *J Neurosci*. 2001;21:2330–2342.